

# Investigations on the Maximum Permissible Operating Temperature of NH-Fuse-Links for General Purpose (gG)

Christian Kühnel, Stephan Schlegel, Steffen Großmann  
*Technische Universität Dresden, Dresden, Germany*  
*Christian.Kuehnel@tu-dresden.de, Stephan.Schlegel@tu-dresden.de*

**Abstract**— Full-range NH fuse-links (gG) are widely used to protect electrical devices. Current requirements of modern power grids, especially in the context renewable energy, implicate changing load profiles with significantly higher thermal stresses for such fuse-links. Thereby, the operational performance of its fuse-elements depends strongly on the temperature. Currently it is neither known to what extent the maximum temperature of the fuse-elements can be permanently increased during normal operation without compromising the reliability of the NH fuse-link nor how that can be verified or controlled non-destructively in practice. Therefore, the fuse-elements ageing at high thermal stress in normal operation was experimentally investigated as well as the influence of that ageing on the tripping in case of overloads. It could be shown that even a high thermal stress in the solid state of the solder can impair the tripping behavior in case of overloads. Furthermore, limiting temperatures for some of the fuse-elements could be identified. To evaluate the fuse-element's temperature non-destructively, the temperature difference between the fuse-element and the blade contacts was studied with thermal calculation models. It could be shown, that this temperature difference is a characteristic parameter of a fuse-link. Additionally, empirical equations were developed to calculate limiting temperatures for different operating conditions.

**Keywords**—Fuse-element, limiting temperatures, long-term behavior, NH fuse-link (gG), thermal network

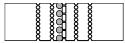
## I. INTRODUCTION

In low-voltage power systems, NH fuse-links for general purpose (gG) are widely used to protect electrical equipment in case of overloads and short-circuit currents. Mainly they are installed in switchgears like fuse-combination units or fuse-switch-disconnectors. In the past, high packing densities within these switchgears and a stronger protection against accidental contact have already led to highly encapsulated installations and an operation at elevated temperatures. Furthermore, the requirements of modern power grids, especially in the context of a growing share of renewable energy, lead to an increasing current load and changing load profiles. If the permissible thermal stress is exceeded in normal operation, accelerated ageing may result. This reduces the service life of the fuse-links and the reliability of the entire switchgear. It is state of the art that the fuse-element's ageing accelerates in normal operation at temperatures above the solidus temperature of the solder [1; 2]. This is caused by the strongly accelerated velocity of the interdiffusion between the solder and the fuse-element at the phase transition of the solder. However, it is not yet known from the literature to what extent the temperature of the fuse-element can be increased up to the solidus temperature of the solder without impairing the reliability of the whole fuse-link. To address these issues, a research project was carried out to determine physically justified limiting temperatures of NH fuse-links that can be used in practice. Initially, the long-term behavior of commercially available fuse-elements was deeply examined with different thermal pre-stressing to identify basic physical reasons for failures and to specify maximum permissible operating temperatures for the fuse-elements. Since these temperatures cannot be easily measured, the temperatures of the fuse-link's blade contacts are recommended as an evaluation criterion [3]. Thus, models were built to calculate the heating of real fuse-links under varying operating conditions. Using these models, the correlation between the temperature rise of the fuse-element and the blade contacts was examined. In this paper, the main results concerning the long-term behavior of fuse-elements and the thermal behavior of fuse-links are presented. Furthermore, a method is derived from those results to determine physically justified limiting temperatures for NH fuse-links in practice.

## II. INVESTIGATED FUSE-LINKS AND CORRESPONDING FUSE-ELEMENTS

Four different commercially available NH fuse-links and its corresponding fuse-elements were investigated. All fuse-links had the same characteristic parameters (application category gG, size NH 2,  $U_r = 500$  V(AC),  $I_r = 250$  A), but differed on the quantity of integrated fuse-elements. Thus, the fuse-elements' geometry and cross-section varied considerably, too. The fuse-elements itself were made out of copper as the base material and contained different tin based solder alloys (TABLE 1).

TABLE 1: EXAMINED FUSE-ELEMENTS

Type	A	B	C	D
Geometry (not scaled)				
Quantity per Fuse-Link	3	2	2	3
Base Material	Cu	Cu, silver plated	Cu	Cu
Solder Alloy	SnBiCu	SnAg	SnCu	SnCd
Solders Melting Range	(165-215) °C	221 °C	227 °C	(180-195) °C

### III. SUMMARY OF THE IMPACT OF AGING IN THE SOLID STATE OF THE SOLDER ON THE FUSE-ELEMENT'S PERFORMANCE IN NORMAL OPERATION AND IN THE RANGE OF SMALL OVERLOADS

Previous investigations have already pointed out, that the physical mechanisms of interdiffusion at the area of the solder depot and the oxidation of the solder itself can be estimated as the main ageing mechanisms in normal operation for the full-range fuse-elements with the application category gG [4]. Due to the ageing, failures like an unintended tripping or even a failed tripping can result. To examine this kind of ageing in normal operation, fuse-elements have been heat-treated in ovens as well as joule heated by AC (50 Hz). According to the individual solder's melting range, the fuse-elements were pre-stressed for 10.000 h at various temperatures up to the solidus temperature of the solder [5; 6]. Furthermore, the effect of that ageing on the performance of the fuse-elements in normal operation and on the tripping behavior in the range of small overloads was examined [7]. Thereby, temperature rise test at rated current as well as the non-fusing and fusing test were carried out with the aged fuse-elements in a simplified fuse-link model. The occurred changes due to ageing were evaluated based on the measured temperature of the fuse-elements in the area of the constriction with the solder and the melting time  $t_s$ . It could be shown that even a continuous operation at high temperatures below the solidus temperature of the solder can impair the fuse-element's performance significantly. The results of these tests showed some strong changes of the tripping like shortened melting times as well as greatly extended melting times. Furthermore, the maximum temperatures of the fuse-elements while tripping increased sharply in some cases or even exceeded the fuse-element's melting temperature. Since the solder is used to enable a tripping at lower temperatures than the melting temperature of the fuse-element, this behavior can be evaluated as a failed tripping. To analyze the observed effects more deeply, further tripping tests were carried out with fuse-elements, which have been pre-stressed at the same temperatures and for the same times but in an inert atmosphere ( $N_2$ ) to distinguish between the effects of interdiffusion and oxidation. Furthermore, metallographic examinations of the aged fuse-elements at the interface between fuse-element and solder were investigated and the thickness of the intermetallic layers was measured at several specimens. Finally, the observed effects were verified by selected tripping tests with pre-stressed real fuse-links. The most important results of all examinations shall shortly be summarized below.

#### A. The oxidation of the solder

After the pre-stressing of the fuse-elements, in most cases a closed oxide film could be observed at the surface of the solder, which protects the remaining solder against a continuous oxidation. Thus, the oxidation does not influence the ageing of the fuse-element significantly. However, the solder should not be positioned partially or completely on the constriction. It could be determined that in such a case the locally inhomogeneous temperature distribution supports a rupture of the oxide films, due to higher thermal induced mechanical stresses. This can result in a complete oxidation of the solder in normal operation [7]. The influence on the performance of the fuse-element in normal operation is negligible, since the influence of the solder on the electrical resistance is very small. However, an overcurrent can no longer be reliably interrupted without solder, so that a failed switching results.

#### B. The interdiffusion at the interface between fuse-element and solder

After the pre-stressing of the fuse-elements, a distinct growth of intermetallic compounds (IMC) could be observed at all interfaces between fuse-element and solder. The influence of these IMC layers on the fuse-element's resistance depends strongly on the geometry of the fuse-element and the position of the solder. Nevertheless, up to a permanent thermal stress in the range of (10 ... 20) K below the solidus temperature of the solder the impact on the performance in normal operation was generally assessed as uncritical. The temperature rise of fuse-elements, which were aged in this temperature range, does not differ significantly from the initial state [7]. The effect of the grown IMCs on the tripping behavior in case of overloads was determined as dependent on the IMC's thickness. Thereby, the duration and temperature of thermal pre-stressing is crucial as the growth of IMC follows the Arrhenius law [8]. Two opposing and overlapping effects were identified. Basically, the growth of IMC layers at the interface increases the resistance and the power losses in the area of the constriction with the solder [5]. In case of overloads, the heating of the fuse-element and thus the velocity of the interdiffusion increase, too. The melting times of the investigated fuse-elements were reduced by up to 34 % compared to the initial state [7]. However, a reliable overload interruption was still ensured in all tests. In that case, the ageing in normal operation resulted in a shift of the time-current characteristic to lower currents. This occurs mainly when thin IMC layers have grown at relatively low temperatures (Fig. 1). Following the Arrhenius law, higher thermal stress in normal operation results in an increased velocity of interdiffusion. Thereby, thicker IMC layers can grow, which additionally influence the concentration profile at the interface. In case of overloads and an already liquid solder, these

thick IMC layers act as an additional barrier between the liquid solder and the fuse-element. Due to their higher melting temperatures [9], they slow down the velocity of the interdiffusion again and thus increase the time until the complete dissolution of the fuse-element. The parallel effect of the increased heating is counterbalanced. With increasing thickness of the IMCs this barrier effect becomes predominant (Fig. 1). The melting time of the investigated fuse-elements were partly increased by 50 % till 250 % compared to the initial state [7]. Furthermore, the maximum temperatures of the fuse-elements while tripping increased sharply in some cases or even exceeded the fuse-element's melting temperature. In those cases, a reliable overload interruption was no longer ensured. It could be shown that very thick IMCs can also cause a failed tripping of the fuse-element. Thereby the characteristics of these effects are largely determined by the individual material combination of fuse-element and solder and the applied thermal stress in relation to the solders melting temperature. In addition, the tripping behavior depends on a large number of other parameters, such as the construction of the fuse-element, especially of its constrictions, and the fuse-link, which can also influence the long-term behavior, but which were not considered in the investigations carried out. The long-term behavior of the fuse-elements could therefore not be conclusively clarified for all investigated types. Based on the gained results, limiting temperatures for a reliable and stable long-term behavior at continuous high thermal stresses could be determined for only some investigated fuse-elements (Fig. 7). Due to a very different dimensioning of the investigated fuse-elements, the potential limiting temperatures can range from < 130 °C up to 200 °C.

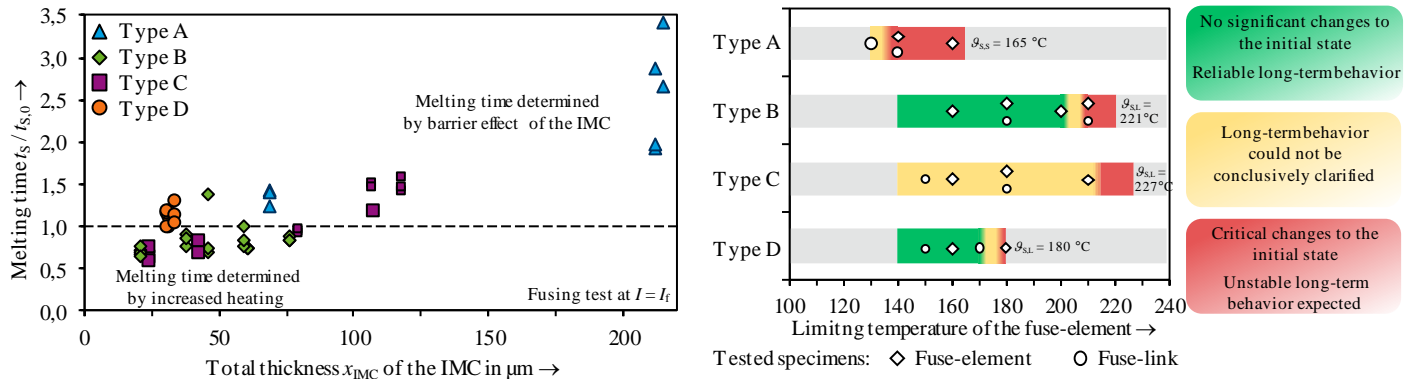


Fig. 1: Melting time  $t_S$  of the aged fuse-element related to the melting time  $t_{S,0}$  in the initial state depending on the total thickness  $x_{IMC}$  of the IMCs at the interface ( $x_{IMC}$  and  $t_S$  measured at different specimens but with the same pre-stressing) Fig. 2: Overview about the experimental results about the long-term behavior and limiting temperature of the investigated fuse-elements and fuse-links at permanently high thermal stress in normal operation

#### IV. THE TEMPERATURE DIFFERENCE BETWEEN FUSE-ELEMENT AND BLADE CONTACTS

##### A. Modeling the temperature distribution of fuse-links under steady-state load conditions

In order to study the correlation between the temperature rise of the fuse-element and the blade contacts, the heating of the fuse-links was computed at steady-state load conditions using the thermal network method (TNM). The TNM is an iterative calculation method, which is based on the analogy between the electric and thermal flow field. To compute the heating, the total heat flow from all heat sources  $P_{loss}$  to points of known temperatures, usually the ambient temperature  $\vartheta_A$ , needs to be modeled in a thermal equivalent circuit (Fig. 3). For this, the components are subdivided into n suitable sections. All thermal processes between these sections need to be described with the basic elements of the TNM (Fig. 3) [10].

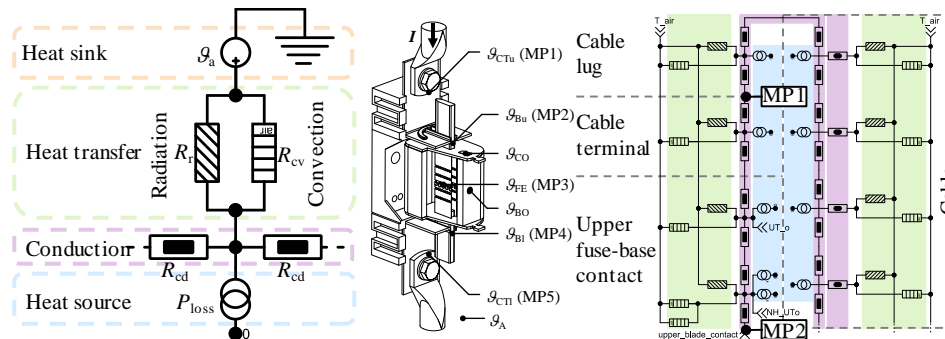


Fig. 3: Basic structure and elements of a simple thermal network Fig. 4: Schematic of the computed test-setup and the thermal network of the upper part of the fuse-base and cable (section)

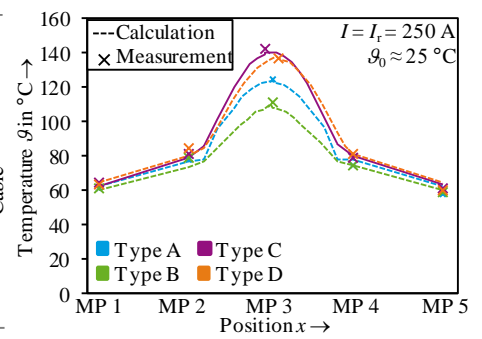


Fig. 5: Calculated and measured temperature distributions of the investigated fuse-links

One of the built models describes the heating of a fuse-link, which is mounted in an open fuse-base and connected to insulated cables according to DIN EN 60269-1:2015 [11]. The thermal network of the fuse-links, which models the heat conduction from the fuse-elements up to the blade-contacts and the outer surface of the ceramic body, is based on an already existing model [4]. Due to the basic

design of fuse-links of the NH-system is very similar, that model could be adapted to the investigated fuse-links by changing geometry and material parameters only. The thermal model of every fuse-link was compiled to an independent single network element. Thus, the fuse-links can easily be interchanged within the same thermal network or they can be used in other thermal models, too. From the surface of the ceramic body, the heat is transferred over radiation and convection to the ambient and the fuse-base. Furthermore, heat is conducted along the current path from the blade contacts over the fuse-base into the connected cables (Fig. 4). The electrical and geometric parameters, which were necessary to calculate the elements of the network, have been measured directly at the corresponding component. All other parameters have been taken from literature [10]. To verify the built models, temperature rise tests were carried out with all four types of fuse-links according to DIN EN 60269-1:2015 [11]. Measured and calculated temperatures are in good agreement (Fig. 5), so that the real temperature distribution of the fuse-link can be modeled with a good accuracy.

### B. Determination of the fuse-link's temperature difference

With the described thermal network, parameter studies were carried out to examine the influence of important boundary conditions on the temperature difference  $\Delta\vartheta$  between the fuse-element and the blade contact: Ambient air temperature  $\vartheta_A$ , temperature of the upper and lower cable terminal  $\vartheta_{CTu}$  and  $\vartheta_{CTl}$  (according to Fig. 4) and current load  $I$ . To minimize the impact of a non-uniform heating of the blade contacts, mainly due to external heating, the temperature difference  $\Delta\vartheta$  is always calculated using the average temperature of both blade contacts (equation (1)). If a relatively uniform heating of the blade contacts is expected, the difference  $\Delta\vartheta$  can also be determined by using one blade contact only.

$$\Delta\vartheta = \vartheta_{FE} - \frac{\vartheta_{Bu} + \vartheta_{Bl}}{2} \quad (1)$$

Firstly, the temperature rise of the cable terminals was varied. Meanwhile, the load current and the ambient temperature were kept constant. Thereby, the temperature difference  $\Delta\vartheta$  remains approximately constant, too (Fig. 6, left). Within the examined temperature range, the temperature difference  $\Delta\vartheta$  increases by a maximum of 5 % for all fuse-links. Thus, the temperature profile along the current-path of the fuse-link does not change qualitatively. It is just shifted to higher temperatures. The higher the temperature of the cable terminals, the lower the heat flow that can be axially dissipated from the fuse-link to the fuse-base (Fig. 6, left). As the overall temperature profile of the fuse-link is raised, the temperature of the ceramic body also rises. The radial thermal resistance between the fuse-link and the ambient is reduced and increasingly more heat can be dissipated via radiation and convection. The improved radial heat dissipation counteracts a steeper temperature profile of the fuse-link due to higher power losses and lower axial heat dissipation. Hence, the temperature difference  $\Delta\vartheta$  can be considered as in good approximation as independent of the temperature rise of the fuse's connections.

By analyzing the influence of the ambient temperature  $\vartheta_A$  at a constant current load  $I_r$ , a linear dependency of the temperature difference  $\Delta\vartheta$  can be determined (Fig. 6, right). The total power losses of the fuse-link increase with the temperature coefficient of the fuse-element's electrical resistance. For copper, that temperature coefficient is  $\alpha_{T,Cu} = 0,0039 \text{ K}^{-1}$  [10]. The ratio of axial to radial heat flow changes very slightly by temperature. The axial heat flow rises due to an increasing temperature gradient along the blades. The heat transfer through convection decreases slightly with higher ambient temperature. According to the strong temperature dependency of the Stefan–Boltzmann law, the heat transfer through radiation increases above average. Thus, the ratio of the radial heat transfer to axial heat dissipation increases a little. Therefore, the temperature dependency of the temperature difference  $\Delta\vartheta$  from the ambient temperature  $\vartheta_A$  is slightly lower than that of the total power losses (Fig. 6, right). By defining  $\vartheta_{A,FL}$  as the ambient air temperature of the fuse-link,  $\vartheta_{FL,20}$  as the specific temperature difference of that fuse-link at  $\vartheta_{A,FL} = 20 \text{ }^\circ\text{C}$  and  $\alpha_{T,FL}$  as the temperature coefficient of the temperature difference, this dependency can generally be expressed by a linear approximation:

$$\Delta\vartheta_{FL}(\vartheta_{A,FL}, I = I_r) = \vartheta_{FL,20} (1 + \alpha_T (\vartheta_{A,FL} - 20 \text{ }^\circ\text{C})) \quad (2)$$

Thereby,  $\Delta\vartheta_{FL}$  is the temperature difference of a fuse-link at a steady-state load at rated current and an ambient temperature of  $\vartheta_{0,FL}$ . The temperature difference  $\Delta\vartheta_{FL}$  differs considerably between the investigated fuse-links (Fig. 7). At  $20 \text{ }^\circ\text{C}$  it ranges from  $\Delta\vartheta_{FL,20} = 33,6 \text{ K}$  for type B till  $\Delta\vartheta_{FL,20} = 59,5 \text{ K}$  for type C. It is mainly determined by the geometry and position of the constrictions along the fuse-element, the construction of the fuse-link and the thermal conductivity of the sand filler. The temperature difference  $\Delta\vartheta_{FL}$  is therefore a specific property of a fuse-link. The temperature dependency of that difference, however, is the same for all four fuse-links. The temperature coefficient was determined to be  $\alpha_{T,FL} = 0,0032 \text{ K}^{-1}$ . As mentioned before, it is mainly defined by the temperature coefficient of the fuse-element's material and the temperature dependency of the ratio of axial to radial heat dissipation.

With equation (2) and the current dependency of the temperature difference  $\Delta\vartheta$ , which was found to meet equation (3), the general temperature difference  $\Delta\vartheta$  of the fuse-links can be determined empirically using equation (4).

$$\Delta\vartheta \sim I^n \text{ with } n = 2,4 \quad (3)$$

$$\Delta\vartheta(I, \vartheta_{A,FL}) = \Delta\vartheta_{FL}(\vartheta_{A,FL}) \cdot \left(\frac{I}{I_r}\right)^{2,4} \quad (4)$$

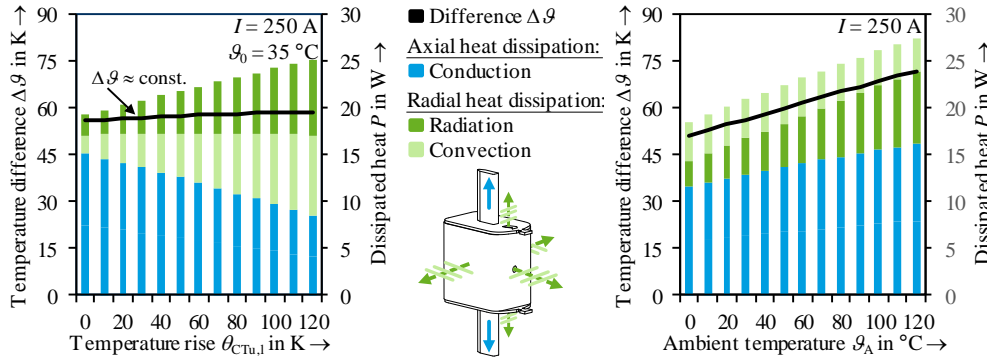


Fig. 6: Temperature difference  $\Delta\theta$  and dissipated heat  $P$  as a function of the temperature rise of the fuse's upper and lower cable terminal  $\theta_{T}$  (left) and the ambient temperature  $\theta_A$  (right); results of type D are shown

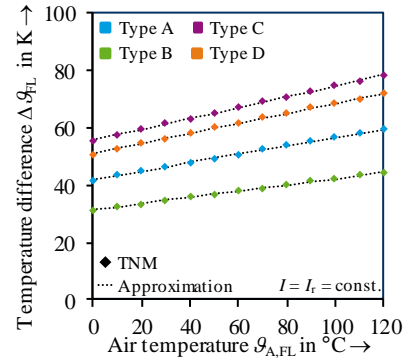


Fig. 7: Temperature difference  $\Delta\theta_{SE}$  dependent of the fuse-link's air temperature  $\theta_{A,FL}$

In further investigations, the heating of the fuse-links inside a fuse-switch-disconnector has also been experimentally examined and computed with the TNM. Thereby, the fuse-switch-disconnector was mounted in a closed cable distribution cabinet. The results showed that equation (4) is principally valid in good approximation for this operation at reduced heat transfer, too. Only the temperature  $\theta_{A,FL}$  needs to be adapted to the different operating conditions. Due to the encapsulated installation of the fuse-link, the air temperature, which surrounds the fuse-link directly, is much higher than the ambient temperature of the cable cabinet. For a suitable determination of the temperature difference  $\Delta\theta$ , therefore, the temperature  $\theta_{A,FL}$  in equation (2) needs to be replaced by the temperature of the air in direct vicinity of the fuse-link at the most unfavorable load condition, where the highest thermal stresses for the fuse-links are expected. For the examined use case, this load condition has been identified as follows: maximum ambient temperature of  $\theta = 35 \text{ }^{\circ}\text{C}$  [11], [12], the fuse-link is loaded with its rated current, the temperature of the bus bar reaches its limit value of  $\theta_{busbar} = 140 \text{ }^{\circ}\text{C}$  [12] and the air temperature inside the cable cabinet is  $\theta_{A,cabinet} = 60 \text{ }^{\circ}\text{C}$ . In that case, maximum temperatures of the air  $\theta_{A,FL}$  above  $100 \text{ }^{\circ}\text{C}$  were computed with the verified model (see Fig. 9).

### C. Determination of the maximum permissible operating temperature

With the combination of the physically justified limiting temperatures  $\theta_{FE,max}$  of the fuse-elements (Fig. 2) and the temperature difference  $\Delta\theta(I, \theta_{A,FL})$ , maximum permissible operating temperatures  $\theta_{B,max}$  for the blade contacts can be derived:

$$\theta_{B,max} = \theta_{FE,max} - \Delta\theta(I, \theta_{A,FL}) \quad (5)$$

As well as the temperature difference  $\Delta\theta$ , these limit values are load-dependent, too. By using the limit temperatures  $\theta_{B,max}$  of the fuse blades as an evaluation criterion, the maximum permissible current load  $I_{max}$  for a reliable and long-term stable operation can be determined (Fig. 8). The results even show, if the temperature  $\theta_{A,FE}$  in equation (2) is adapted to the individual operating condition, the maximum permissible load can as well be determined in good approximation for use cases with reduced heat transfer. The temperature  $\theta_{A,FE}$  can therefore also be regarded as a parameter, which qualifies the thermal stress of a fuse link in a particular use case.

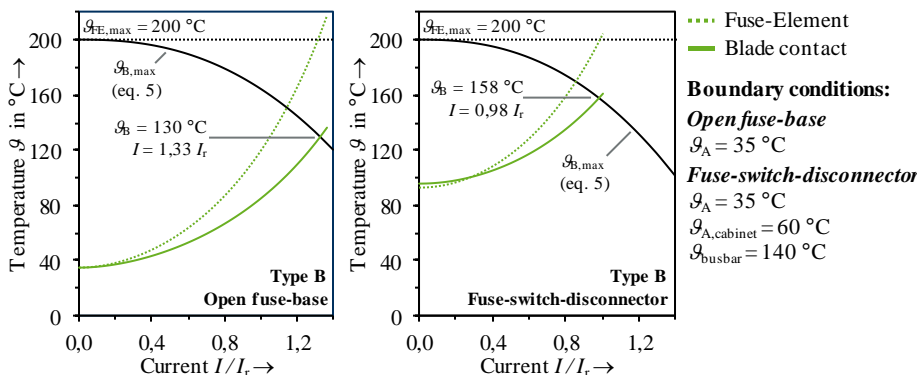


Fig. 8: Determination of the maximum permissible load of the fuse-link based on the equation (5) and depending on the operating condition (illustrated by the example of fuse-link type B)

Type	A	B	C	D
$\theta_A$ in $^{\circ}\text{C}$	35			
$\Delta\theta_{FE,20}$ in K	35,0	33,6	59,5	54,7
$\theta_{FE,max}$ in $^{\circ}\text{C}$	130 <sup>a</sup>	200	160 <sup>a</sup>	170
<b>Open fuse-base according DIN EN 60269-1:2015</b>				
$\theta_{A,FE}$ in $^{\circ}\text{C}$ (for eq. (2))	35			
$\theta_{B,max}$ in $^{\circ}\text{C}$	86	130	94	102
$I_{max}$ in A	0,98 $I_r$	1,33 $I_r$	1,03 $I_r$	1,08 $I_r$
<b>Fuse-switch-disconnector in a cable distribution cabinet</b>				
$\theta_{A,FE}$ in $^{\circ}\text{C}$ (for eq. (2))	113 <sup>b</sup>	113 <sup>b</sup>	118 <sup>b</sup>	113 <sup>b</sup>
$\theta_{B,max}$ in $^{\circ}\text{C}$	114	158	127	133
$I_{max}$ in A	0,58 $I_r$	0,98 $I_r$	0,70 $I_r$	0,76 $I_r$

<sup>a</sup> unfavorable load case with TNM:  $\theta_{A,cabinet}=60^{\circ}\text{C}$ ,  $\theta_{busbar}=140^{\circ}\text{C}$ ,  $I = I_r$ ,  $L1$

Fig. 9: Boundary conditions and limit values for the maximum permissible load of the investigated fuse-links

Despite the same characteristic parameters of the fuse-links, its maximum permissible temperatures and load currents differ greatly (Fig. 9). High limiting temperatures of the fuse-element in combination with a small characteristic temperature difference  $\Delta\theta_{FE,20}$  of the fuse-link therefore result in a higher permissible current load and a higher thermal endurance, respectively. The current technical guideline

DIN CLC/TR 60269-5:2012 [3] recommends limit temperatures for the blade contacts in case of a reduced heat transfer of  $\theta_{B,max} = 100\text{ }^{\circ}\text{C}$  for continuous operation. However, due to the load dependency of the temperature difference  $\Delta\theta$  (eq. (4)), the determined limiting temperatures are significantly higher for all investigated fuse-links and range from  $114\text{ }^{\circ}\text{C}$  up to  $158\text{ }^{\circ}\text{C}$ , depending on the fuse-links dimensioning (Fig. 9). Thus, especially for use cases with continuous high thermal stress, an individual limit value for each fuse-link is recommended in order to achieve an optimal utilization of the components.

## V. CONCLUSION AND OUTLOOK

Within this paper, the long-term behavior of full-range fuse-links at continuous high thermal stress was examined. It has been established that even a continuous operation of fuse-links at high temperatures below the solidus temperature of the solder can result in a significant ageing of its fuse-elements. This can compromise the performance of the fuse-link mainly in the range of small overloads. Up to temperatures in the range of (10 ... 20) K below the solidus temperature of the solder the performance of the investigated fuse-elements in normal operation is usually not significantly influenced. The ageing of the fuse-elements at temperatures below the solidus temperature of the solder is mainly caused by the interdiffusion at the interface between the solder and the fuse-element. Depending on the thickness of IMC layers at the moment of the occurring overload, melting times can be either shortened or greatly extended. Thin IMC layers usually shift the time-current characteristic to lower currents and an unintended tripping may result. However, a reliable overload interruption is still ensured. The thicker the IMC layers are, the more they act as an additional barrier at the interface and increase the melting times. That causes higher thermal stress during the tripping and can even cause the tripping to fail. Based on those results, limiting temperatures could be derived for some of the investigated fuse-elements, which ensure a reliable long-term performance. Those limiting temperatures for fuse-element essentially depend on the solidus temperature of the solder as well as on the material combination of fuse-element and solder. Due to a very different dimensioning of the investigated fuse-elements, potential limiting temperatures can range from  $< 130\text{ }^{\circ}\text{C}$  up to  $200\text{ }^{\circ}\text{C}$ .

Furthermore, thermal models were built and verified, to study the correlation between the temperature of the fuse-element and the blade contacts of the fuse-link for different use cases. It was shown that this temperature difference for different use cases is in good approximation independent of the temperatures of the fuse's connections. It only depends on the air temperature in the direct vicinity of the fuse link as well as on the load current. Further, it could be found out that the specific temperature difference between the fuse-element and the blade contacts can basically be considered as a characteristic parameter of a fuse link, which is mainly determined by its material properties and construction. Together with the examined limiting temperatures of the fuse-elements, empirical equations were developed, which allow for a calculation of physically justified limiting temperatures for the blade-contacts in different operating conditions. The determined limiting temperatures are generally load-dependent. Despite the same ratings, the limit values differ significantly between the investigated fuse-links. Nevertheless, even at challenging operating conditions like the operation in a fuse-switch-disconnector with strongly reduced heat transfer, the permissible limiting temperatures are higher than the recommendations of the guideline DIN EN 60269-5:2012 [3]. The presented method allows a non-destructive evaluation of the fuse-element's thermal stresses in practical operating conditions. In further investigations, especially the specific temperature difference between fuse-element and blade contacts as well as its temperature dependency should be investigated more deeply for other sizes and rated currents of NH fuse-links. By knowing these correlations, the presented method could be a useful tool for the development of fuse-links in future and can help to determine the maximum load in standardized tests.

## VI. ACKNOWLEDGEMENT

The authors thank NH/HH-Recycling e.V. and its industrial partners for the support of this project and the excellent cooperation.

## VII. REFERENCES

- [1] Klepp, G. Über das Abschmelzverhalten von Sicherungsschmelzleitern im Überlastbereich, Dissertation, Braunschweig 1982
- [2] Hofmann, M. Experimentelle und rechnerische Untersuchung von Ansprechennlinien und Alterungsvorgängen bei Sicherungsschmelzleitern, Dissertation, Braunschweig, 1987.
- [3] DIN CLC/TR 60269-5:2012 Niederspannungssicherungen - Teil 5: Leitfaden für die Anwendung von Niederspannungssicherungen.
- [4] Kühnel, C.; Schlegel, S.; Großmann, S. Untersuchungen zur Überlastabschaltung von Ganzbereichssicherungen bei erhöhter Sammelschienen- und Umgebungstemperatur. 22. Fachtagung Albert-Keil-Kontaktseminar, 09.-11.10.2013, Karlsruhe, VDE Verlag GmbH, Berlin 2013, S. 133–142.
- [5] Kühnel, C.; Schlegel, S.; Großmann, S. The influence of important ageing mechanisms on long-term behavior and reliability of fuse-links at higher temperatures. 10th International Conference on Electric Fuses and their Applications, 14.-16.09.2015, Dresden, S. 157–164, <https://www.nh-hh-recycling.de/id-2015-icefa-dresden.html>.
- [6] Kühnel, C.; Schlegel, S.; Großmann, S. Investigations on the Long-Term-Behavior and Switching Function of Fuse-Elements for NH-Fuse-Links (gG) at Higher Thermal Stress. 6th International Youth Conference on Energy (IYCE), 21.-24.06.2017, Budapest.
- [7] Kühnel, C.; Schlegel, S.; Großmann, S. Grenztemperaturen für NH-gG-Schmelzleiter im modernen Energieversorgungsnetz. 24. Fachtagung Albert-Keil-Kontaktseminar, 11.-13.10.2017, Karlsruhe. VDE Verlag GmbH, Berlin, S. 189–197.
- [8] Shewmon, P. Diffusion in Solids. Second Edition. Springer International Publishing, Cham 2016.
- [9] Massalski, T. B.; Okamoto, H. Binary alloy phase diagrams. ASM International, Ohio 1990.
- [10] Böhme, H. Mittelspannungstechnik. Schaltanlagen berechnen und entwerfen. 2., stark bearb. Aufl. Huss-Medien Verl. Technik, Berlin 2005.
- [11] DIN EN 60269-1:2015 Low-voltage fuses - Part 1: General requirements (german version).
- [12] DIN EN 61439-1:2012 Low-voltage switchgear and controlgear assemblies - Part 1: General rules (german version).